Optimal Generation Dispatch With High Penetration of Photovoltaic Generation

Sara Eftekharnejad, *Member, IEEE,* Gerald Thomas Heydt, *Life Fellow, IEEE,* and Vijay Vittal, *Fellow, IEEE*

***Abstract*—Power system operation practices are changing with the addition of renewable energy resources such as photovoltaic (PV) sources. The diverse and intermittent nature of these resources demands new operation strategies to ensure system reliability. As more PV units are added to power systems, the power generated by conventional generation resources should be reduced to accommodate these new resources. The reduction in fossil-fired generation allows realization of benefits in the sustainability of the generation mix. While some of the conventional generating units are retired, some should be retained for system reliability. This paper investigates the impact of generation redispatch or generation displacement in systems with high PV penetration. Comparing various study scenarios, a method based on regression techniques and Chebyshev's inequality is introduced in this paper. This method is used to calculate the dispatch or displacement ratio of the conventional generators for optimal steady state and transient response of the system. Recommendations are formulated based on an actual large-scale power system in the western United States.**

***Index Terms*—Chebyshev inequality, converter, distributed power generation, generation dispatch, photovoltaic (PV) generation, power system stability.**

I. Introduction: Addition of PV Generation Resources

THE NEED to replace fossil fuel generation resources with clean and renewable energy resources has initiated renewable portfolio standards (RPSs) that have created new challenges for power grids. As a result of the new mandates, various jurisdictions are expected to increase their level of renewable generation such as photovoltaic (PV) and wind resources in the near future [1]. The rapid increase in these alternative generation resources has resulted in unprecedented structural changes in power grids. Supplying the loads from distributed resources closer to the loads is one example of the changes occurring in contemporary power systems.

Presently, practiced standards such as IEEE 1547 [2] do not allow residential and rooftop PV inverters to regulate voltages at the point of common coupling. This limitation has caused the PV installations to be operated at fixed power factor and, in the majority of the cases, at unity power factor. Operating rooftop PVs mainly as sources of active power results in characteristics such as low-system inertia and potentially insufficient reactive power reserves in systems with high penetration of PV resources. Given these characteristics, power systems encounter an increased need for reactive power as well as active power reserves. As more PV units are added to the existing grids, the output power generated from the other units should be suitably adjusted to maintain a generation and load balance. However, in practice, it is not economically and environmentally justifiable to retain the more expensive units and all the fossil fuel units in service. Therefore, displacing a portion of the conventional generators with PV systems is an inevitable consequence of high PV penetration. As a result of these generation displacements, the ability to respond to various system transients will increasingly transfer the burden on the nondisplaced conventional generators.

Recent studies have analyzed the effect of high PV penetration on power system transmission and distribution systems [3]–[7]. The authors in [3] have investigated the impact of high PV penetration on power system voltage stability as well as transient stability. Studies carried out so far on the system with high PV penetration illustrate that the impact of high PV penetration on existing systems can be impacted by a spectrum of factors. The locations as well as the type of the PV resources, availability of adequate reserves within the system, the generators displaced by PV generation resources, and the generators being dispatched as a result of high PV penetration are among the factors that can change the severity of the impacts of high PV penetration on system behavior. Although all these factors contribute to PV impacts, some factors may overshadow others due to the extent and type of impact on system behavior. With higher penetration of PV resources, the strategy used to displace or reschedule the conventional generators becomes one of the critical factors of power system operation—and the details of the displacement presents a question yet to be answered in full. An appropriate selection of the displaced generators as well as the generators whose outputs are only "backed down" rather than entirely displaced by PV units is essential for mitigating the adverse effects of the PV systems on the power grid. This issue has first been raised in [8], in which the impact of unit commitment on the frequency response of the system was investigated.

The literature of power system economic operation dispatch is large and extensive. The objective of these works [9], [10] is to identify the optimal dispatch with respect to operation cost or system constraints. More recent works [11]–[13] have also studied the impact of distributed energy resources on real-time dispatch of the conventional generation as well as optimal dispatch of the alternate resources.

To ensure system reliability and to decrease the adverse effects of these unprecedented changes on existing grids, there is an imminent need to identify the optimal dispatch or displacement

Manuscript received October 09, 2013; revised April 23, 2014; accepted May 25, 2014.

S. Eftekharnejad is with Tucson Electric Power Co., Tucson, AZ 85701 USA (e-mail: sara.eftekharnejad@ieee.org).

G. T. Heydt and V. Vittal are with the Department of Electrical, Computer, and Energy Engineering, Arizona State University, Tempe, AZ 85287 USA (e-mail: vijay.vittal@asu.edu; heydt@asu.edu).

Color versions of one or more of the figures in this paper are available online at http://ieeexplore.ieee.org.

Digital Object Identifier 10.1109/TSTE.2014.2327122

ratio of the conventional generators that lead to reliable system operation. In this context, the displacement ratio is the ratio of power generation [megawatts (MW)] removed from the generation pool versus the generation (MW) that is simply redispatched. It is critical to analyze the system response under various displacement ratios.

This work studies a large system that is part of the U.S. Western Electricity Coordinating Council (WECC) and demonstrates the need for an *optimal dispatch ratio* (ODR). In addition to developing an approach to determine ODR, the optimal displace/dispatch ratio of the conventional generators is also evaluated while more PV generation is added to the system. Various parameters are monitored to determine satisfactory system performance. Frequency of operation and bus voltages are among the parameters monitored in this paper.

This paper is organized as follows. In Section II, a brief description of the studied system with high PV penetration is presented. Section III illustrates various scenarios of dispatch ratio (DR) and their impact on the aforementioned system. Section IV introduces a method for calculation of the ODR value. Simulation results are presented in Section V, followed by the conclusion in Section VI.

II. Characteristics of the Test Bed System

A. Studied Test Bed

To demonstrate the applicability of the methods and recommendations presented in this work, a large system is being selected as the test bed for this study. The studied system, which consists of 2420 buses and 1860 transmission lines and 226 generators, is part of the WECC system with a mixed combination of generation resources. The total generation being provided by conventional generation resources is 21 GW and the load is 13 GW. As stated in [3], light load conditions may lead to high voltage magnitudes with high PV penetration levels. For this reason, the test bed system has been chosen to have loads representing the light load operating conditions.

To illustrate a case study with high PV penetration, a 40% PV penetration, i.e., 8033 MW, mainly supplied by rooftop PVs is considered. The PV penetration is defined as the percentage of the total power supplied by the PV resources over the total power supplied by all the generation resources within the studied system. This level of PV generation is approximately equivalent to 13% PV penetration by energy, which is below RPS targets for many U.S. states. The PV systems are modeled as constant current loads and at unity power factor. Although, in reality, some portion of PV systems would be utility scale and would have voltage regulation capabilities, for the purpose of this work and to emphasize the importance of DR a conservative approach is adopted. The PV systems are aggregated at 69-kV buses based on a substation map of the system.

B. Study Base Cases

As stated, the objective of this paper is to show how different DRs would impact system reliability with increased PV penetration and lower inertia in the system. It is critical to analyze the system to calculate for each MW addition of PV generation, the percentage of generation compensated by displacing conventional units and the percentage of generation compensated by a reduction in the generated output of the in-service units. Therefore, the described test bed is modified, and different study cases are created for various DRs.

To create the aforementioned power flow files, the first step is to identify the base case generators that are expected to be *displaced* by the PV units as well as those that are being *dispatched*. Also, the third category of generators relates to the *base generation* that is not impacted by the addition of the PV units. Therefore, conventional generators are classified into three main categories: 1) dispatched; 2) displaced; and 3) base generators. For a 40% PV penetration case, 8033 MW of active power is assumed to be supplied from the residential rooftop and commercial PVs. This active power is compensated by a reduction in conventional generator outputs with various scenarios of dispatch/displace ratios. In total, 21 study cases were created starting from the case with all the power reduction supplied from displacing the conventional generators to Case 21 in which the conventional generators are rescheduled to reduce their cumulative output by 8033 MW. The rest of the cases have various dispatch/displace ratios defined as follows for case i:

$$\begin{aligned}
&\text{Delta} = 0.05\\
&\text{Ratio} = 1 - \text{delta} \times i\\
&0 \le i \le 20\\
&\text{Displace(MW)} = \text{ratio} \times \text{PV}_{\text{MW}}\\
&\text{Dispatch(MW)} = \text{PV}_{\text{MW}} - \text{displace(MW)}\\
&\qquad\qquad = (1 - \text{ratio}) \times \text{PV}_{\text{MW}}. \qquad (1)
\end{aligned}$$

As seen from (1), in each iteration, the displacement ratio is decreased by 5%, and hence the DR is increased by the same amount. It should be mentioned that the output power of the redispatched generators is reduced based on their contribution to the total output power of the dispatched generators. Therefore, the same contribution ratio is retained while decreasing the redispatched generators' output power. The created 21 study cases are used in the following sections to analyze the impact of DR on power system performance during contingencies.

III. Impact of Generation Dispatch on System Transients

Adequate resources at all times are essential for a frequency response that complies with various standards such as North American Electric Reliability Corporation (NERC) performance criteria [14]. Due to the intermittent nature of the PV systems, retaining adequate power resources within the system is essential for secure system operation to account for those variations. To illustrate the impact of various DRs and to calculate the ODR with respect to the frequency of the system, the cases described in the previous section with 40% PV penetration are studied under two common scenarios. The system equivalent frequency, which is adopted from [8] and as defined in (2), is calculated and compared for each of the 21 cases

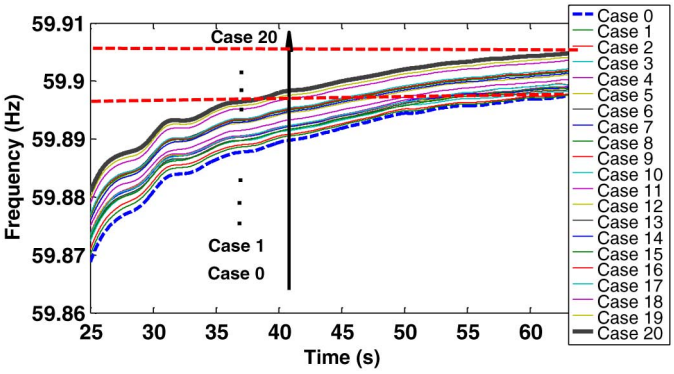

Fig. 1. Frequency settling value of various dispatch ratios for a loss of two major units.

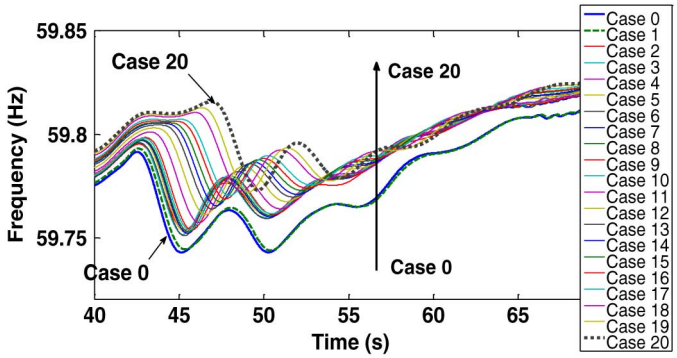

Fig. 2. System equivalent frequency for various dispatch ratios for loss of rooftop PVs and two large utility scale PV units.

$$f_{\text{sys}} = \frac{\sum_{i=1}^{N} \text{MVA}_i \times f_i}{\sum_{i=1}^{N} \text{MVA}_i} \tag{2}$$

where f_{sys} is the MVA-weighted average frequency defined for the entire system, MVA_i is the rating of generator i, f_i is the frequency of generator i, and N is the total number of the synchronous generators in the system.

The first studied scenario compares the frequency response of the system for all different DR scenarios, following a loss of two major units in the study area. The second scenario not only entails loss of the two major units but also assumes a major loss in the output power of the PV units. These variations could be the result of weather fluctuations such as cloud cover, single system event, or other unpredictable weather conditions that commonly occur in systems with high PV solar-based generation. The two cases are then compared to draw conclusions about the ODR with regards to adequate system reserves. The active power exchange to the other areas is maintained constant within this analysis to only study the local effects of PV systems on the studied area.

A. Case 1: Loss of Two Major Units

To account for a considerably large outage, a 2820 MW of conventional power loss from the overall system generation is assumed. Consequently, the system frequency is expected to settle at a lower value than the normal operating frequency, i.e., 60 Hz. All the aforementioned 21 cases with various dispatch or decommitment ratios are utilized for simulation of the case described. It is assumed that the units, whose outage will be equivalent to a total of 2820 MW power loss from the system generation pool, are switched off at $t = 5$ s of the simulation time, whereas the system is operating under normal operating conditions before that time. For each study scenario, the time responses of the frequencies of the conventional generators are simulated and the system equivalent frequency shown in (2) is calculated. Fig. 1 illustrates the settling frequency of the system for the aforementioned scenario. Various dispatch/decommitment ratios are simulated, ranging from zero DR in the first set of data to 100% DR in the 21st scenario. As seen from Fig. 1, the more units that are redispatched rather than displaced, the better would be the system response due to more resource availability.

B. Case 2: Loss of Two Major Units in Addition to Loss of PV Units

Unlike the previous scenario, the second scenario studied does not assume constant availability of the PV units. In fact, the same outage scenario simulated in the previous section is studied in this case, in addition to the assumption of a cloud cover that could impact the output power of the PV units. Similar to the previous case, a penetration level of 40% is assumed for the cases studied. The simulation carried out in this section assumes a 2400 MW of power loss from the total system PV generation. A cloud cover could be an example of those scenarios that can lead to such power outages. It is assumed that this outage occurs after 4 s of the start of the simulation and will continue until 15 s. At $t = 15$ s, the two outaged units will also trip that will add to the outage of the PV units. The simulation is continued until $t = 70$ s in order to observe the settling frequency of each scenario studied. Simulation results are presented in Fig. 2.

By comparing Figs. 1 and 2, it is seen that similar to the previous scenario, the cases have a similar response. However, due to the additional outages in the second scenario, the system is more stressed in the first and second cases, i.e., 0% and 5% DR study cases. If a summer peak case was selected for the study, the results could be different in terms of the active power availability due to the fact that most of the generators are already at their maximum value in the peak case. The lower the frequency drop, the more is the chance for additional outages as a result of the under frequency relays disconnecting additional loads on distribution feeders.

The last two examples illustrate the fact that under certain conditions, various DR values and hence the number of generators that are kept online could impact the system response under certain conditions.

C. Impact of DR on System Response to Disturbances

Lack of inertia is a direct artifact of displacing the generators in the systems with high PV penetration. Various study scenarios with different generation DRs could differ in their responses to the system faults due to varying system inertia. The objective of this section is to identify the *minimum DR*, while achieving an acceptable system behavior in terms of the bus voltages, frequency response, etc. The minimal DR ensures less operating costs and the ability to retire large coal units.

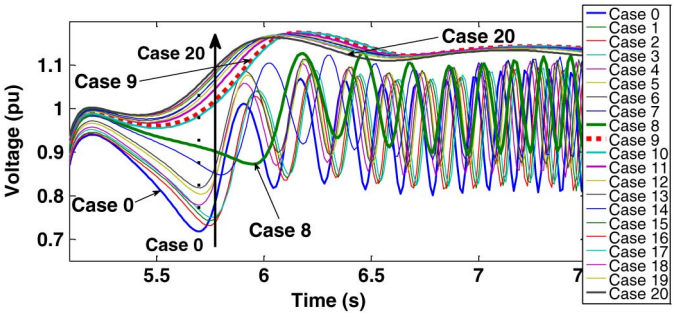

Fig. 3. Voltage magnitude of the faulted 500-kV bus following a three-phase fault.

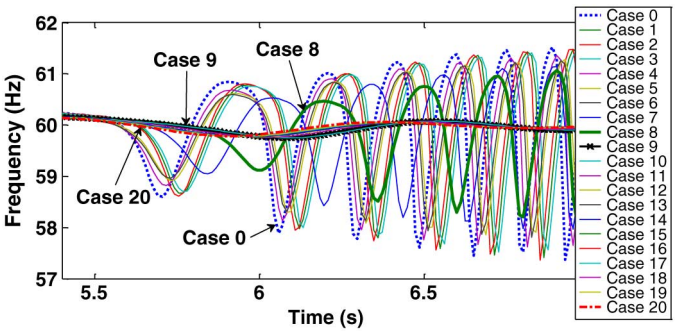

Fig. 4. Frequency of the faulted 500-kV bus following a three-phase fault.

The disturbance studied is a three-phase fault at a 500-kV level bus which is cleared after 5 cycles with a consequent outage of the connecting 500-kV transmission line. The faulted bus is close to three main generating stations. Therefore, a fault at this location can disturb a significant amount of the generated power from these three generating units. Similar to the previous cases studied, a 40% PV penetration case is simulated for all the 21 cases described in the previous sections. Figs. 3 and 4 present the simulation results.

As seen from the bus frequencies and the voltage magnitudes, the system goes unstable following the aforementioned bus fault for certain DRs. The system becomes stable as the DR is increased and therefore less conventional generators are decommitted from the service. The minimum DR that makes the system stable is found to be related to the tenth studied scenario (Case 9) that corresponds to a DR of 45%. This DR means for every 100 MW of PV power added to the system, 45 MW of power generated by the conventional generating units is reduced by redispatching those units and 55 MW of the required power reduction is provided by decommitting conventional units.

In a second scenario, a three-phase fault at another 500-kV bus, which is located in vicinity of generator G1, is simulated. The fault is cleared after five cycles, and the transmission line connecting the two buses is outaged following the fault clearance. Voltage magnitude and frequency of the faulted bus is presented in Figs. 5 and 6, respectively. The voltage magnitude of the generator G1 terminal bus is also shown in Fig. 7.

As seen from Fig. 6, the frequency response of the faulted bus illustrates a better performance as the DRs are increased in the system. However, after a certain DR, the difference between the

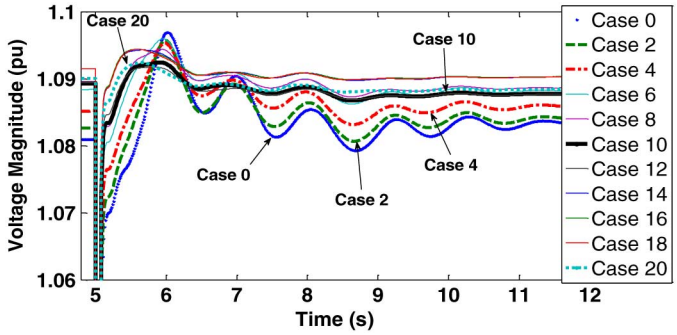

Fig. 5. Voltage magnitude of the faulted bus following the Case 2 disturbance.

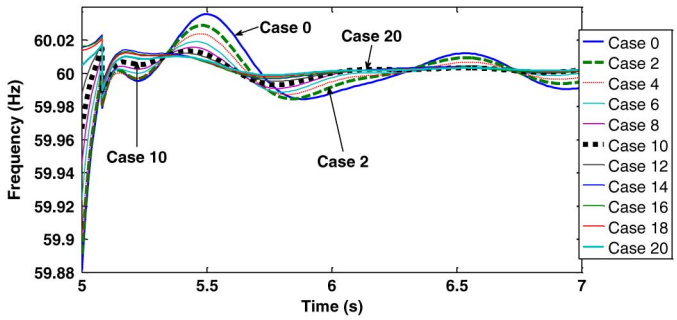

Fig. 6. Frequency of the faulted bus following the Case 2 disturbance.

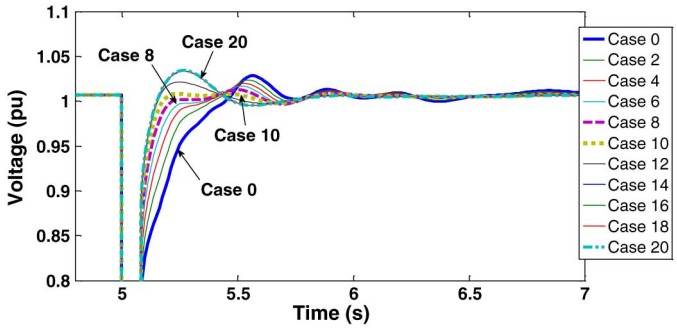

Fig. 7. Voltage magnitude of generator G1 terminal bus following the Case 2 disturbance.

frequency responses becomes insignificant. Other factors such as the bus voltages could be used to determine the ODR in this case.

The voltage magnitude of the faulted bus as shown in Fig. 5 shows a significant improvement at the tenth study scenario. This scenario corresponds to a 45% conventional generation DR or in other words, 55% of the generators are decommitted from the service as PV generation is added to the system. The 45% DR also leads to the best voltage behavior for generator G1 terminal bus as shown in Fig. 7. The voltage magnitude of this bus reaches the smallest peak under the 45% DR following the Case 2 disturbance.

IV. ODR With Regards to Steady-State Performance

Various DRs, translate to a different number of online generators. The difference in the total number of the online generators results in variations of the power flows through the

transmission lines. As the DR decreases (in other words, *displacement ratio increases*), the power resources become more remotely located to the loads. Hence, the bus voltages and line flows may be affected differently with the addition of the PV units while under different DRs.

Simulation results presented in the preceding sections revealed the ODR value based on the transient response of the system. These simulation results illustrate the fact that an ODR exists and should be used for reliable system operation. Although the ODR value calculated based on the transient simulations ensures system reliability during the transients, it will not necessarily yield an optimal system behavior in terms of the steady-state performance. This section introduces a method to calculate the ODR value for the system in order to maintain acceptable steady-state performance. Maintaining bus voltage magnitudes within $\pm 5\%$ of the nominal value and the line flows below the thermal ratings would translate to an acceptable steady-state performance.

The method introduced in this paper estimates the ODR value as a function of the *bus criticality index* (BCI). The BCI is a measure that quantifies the bus voltage magnitude violations and their distances from a tolerance in order to show whether the system buses are operating under critical conditions. The BCI for the bus voltage magnitudes are defined as follows:

$$\mathrm{BCI} = \frac{1}{e}\int_{1}^{|v-1|+1} e^{x-1}dx \times (1 + (1 - P_{\mathrm{critical}})g) \quad (3)$$

$$P_{\mathrm{critical}} = \frac{n_{\mathrm{critical}}}{n_{\mathrm{critical}} + n_{\mathrm{acceptable}}} \quad (4)$$

$$g = \begin{cases} 0, & \text{if} \quad 0.95 < |v| < 1.05 \\ 1, & \text{otherwise} \end{cases} \quad (5)$$

where

v	bus voltage;
n_{critical}	number of times bus voltage is outside the tolerance range for all the historical data;
$n_{\mathrm{acceptable}}$	number of times bus voltage is within the acceptable range for all the historical data.

As seen from (3), the BCI is defined based on the voltage of each bus and consists of two terms. Since the objective of the BCI is to determine the criticality of a bus voltage, the two terms are defined in a manner to increase the BCI value as the voltages deviate from the acceptable tolerance. The tolerance is defined as a voltage between 0.95 and 1.05 p.u. The first term in (3) will serve as an exponential penalty factor as the voltages deviate from 1 (p.u.). The second term is intended to serve as penalty factor for the bus voltage if it is operating within the critical range. Therefore, the function $g(v)$ is only nonzero outside the acceptable voltage range. The function P_{critical} is calculated based on numerous simulations of the study system and represents the probability of criticality based on the test data. The objective, including the second term in (3), is to significantly increase the BCI if the criticality occurs less frequently as a result of a severe contingency. On the other hand, if a particular bus holds a critical voltage value at all times, including the no contingency case, the BCI would be less affected by this particular bus voltage.

The test data utilized to calculate p_{critical} include bus voltages for the entire system, under various DRs, following various contingencies as well as the case with no contingency. To compare the accuracy of the results achieved based on the BCI defined in (3), the term p_{critical} is also calculated based on the *Chebyshev's* inequality [15], [16]. Chebyshev's theorem states that for a random variable x with *any probability distribution function* and finite expected value μ and nonzero variance σ^2

$$\Pr(|X - \mu| \geq k\sigma) \leq \frac{1}{k^2} \quad (6)$$

where Pr is the probability of the random variable x. Equation (6) determines the upper bound for the probability of a random variable to be k standard deviations away from the mean value μ. Based on (6) the modified BCI function is calculated as

$$\mathrm{BCI} = \frac{1}{e}\int_{1}^{|v-1|+1} e^{x-1}dx \times (1 + (1 - P_v)g) \quad (7)$$

$$P_v = \frac{1}{k^2}$$

$$k = \frac{v - \mu}{\sigma}. \quad (8)$$

The parameter μ is the mean value, and σ is the standard deviation of the test data that are collected by the contingency analysis. The term k shows how far, in terms of the number of standard deviations, a particular bus voltage is from the mean value of the historical data of that bus voltage. The BCI values calculated based on (7) are less conservative than those calculated by (3) as they are defined based on the upper bound probability of criticality. Hence, the ODR values found based on the second method would be smaller due to the fact that the probability of criticality is higher most of the times.

A *regression* method is used to estimate the ODR of the system as a function of the bus BCIs, which are functions of system bus voltages. Regression is a tool to predict a real value (the DR) for a given data set such as the bus voltage magnitudes. Regression techniques estimate the relation between a dependent variable y and the independent variables x_i

$$y \approx F(x_1, x_2, \ldots, x_n). \quad (9)$$

Among various regression techniques, *linear regression* in its simplest form represents the output variable y or label, as a linear function of the input variables set X or regressors as follows:

$$y = X\boldsymbol{\omega} + \varepsilon \quad (10)$$

where $\boldsymbol{\omega}$ is the vector of regression coefficients and ε is the error of the linear regression. The objective of each regression method is to estimate $\boldsymbol{\omega}$ and ε using the test data that are often called the *learning data set*. Various methods are applied to solve the regression problems [17], among which weighted least squares (WLS) is a widely used method. The objective of this method is

to minimize the difference between Y and the estimated value as follows:

$$\min \|Y - XW\|^2 \tag{11}$$

$$\frac{\partial}{\partial W}\|Y - XW\|^2 = 0$$

$$\frac{\partial}{\partial W}(Y - XW)^T(Y - XW) = 0$$

$$\frac{\partial}{\partial W}\left(Y^T - W^T X^T\right)(Y - XW) = 0$$

$$\frac{\partial}{\partial W}\left(Y^T Y - Y^T XW - W^T X^T Y + W^T X^T XW\right) = 0$$

$$-2X^T Y + 2X^T XW = 0$$

$$2X^T XW = 2X^T Y$$

$$W = \left(X^T X\right)^{-1} X^T Y. \tag{12}$$

The weight matrix W calculated from (12) determines the relation between the output variable, which is DR in this case, and the regressors, i.e., the BCI values. As seen from (12), calculation of W requires calculation of the inverse of the matrix $(X^T X)$, which often requires extensive calculations. To avoid calculation of the aforementioned matrix inversion, the matrix X can be represented as multiplication of three matrices U, V^T, and the diagonal matrix Σ using the singular value decomposition (SVD) technique as shown in (13)

$$X = U\Sigma V^T$$

$$W = \left(X^T X\right)^{-1} X^T Y = \left(V\Sigma U^T U\Sigma V^T\right)^{-1} V\Sigma U^T Y$$

$$\rightarrow W = \left(V\Sigma^2 V^T\right)^{-1} V\Sigma U^T Y = V\Sigma^{-2} V^T V\Sigma U^T Y$$

$$\xrightarrow{VV^T = I} W = V\Sigma^{-1} U^T Y. \tag{13}$$

Based on the aforementioned methods of calculating the BCI values, for each set of *test data*, the corresponding BCI values are calculated for each bus. These calculated values serve as the regressors for estimating the DR for the studied system. By calculating the estimate of the DR as a function of the bus voltages, the ODR could be found. The ODR ensures that the system criticality index (SCI), which is shown in (14), is minimized. The parameter n is the number of buses in (14)

$$\mathrm{SCI} = \sum_{i=1}^{n} \mathrm{BCI}_i. \tag{14}$$

If the buses hold high-voltages most of the time, the ODR will ensure their magnitudes do not fall into the most severe range of the bus voltages. In other words, by knowing the minimum achievable SCI and finding the DR that results in this value, the ODR is found. Consequently, by calculating the minimum value of the SCI and estimating the DR based on the BCIs of a test case that yields the minimum SCI, the ODR of the system will be obtained as shown in (15). The parameter j is the index of the test case that yields the minimum SCI value among all the test cases

$$\mathrm{ODR} = (\mathrm{BCI}_1, \mathrm{BCI}_2, \ldots, \mathrm{BCI}_n)^j W. \tag{15}$$

A summary of the method proposed to calculate the ODR of the system is shown in Fig. 8.

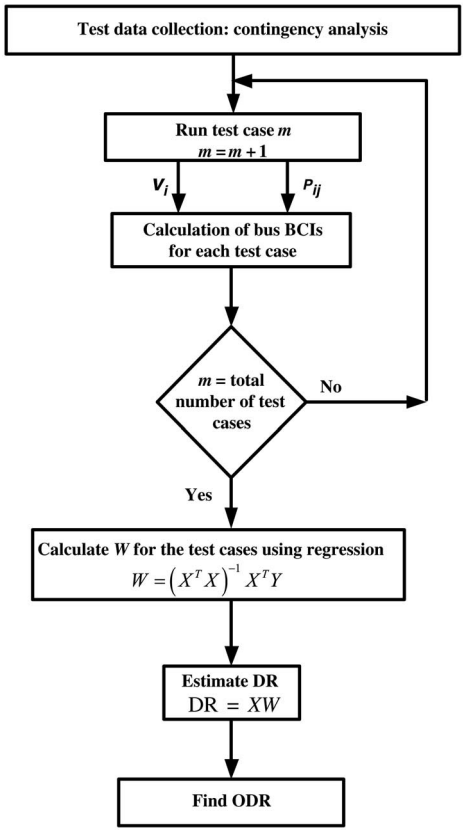

Fig. 8. Flowchart for calculating ODR.

V. Numerical Example

To illustrate the effectiveness of the proposed method, a numerical example is presented in this section for the system described and the corresponding 21 DR scenarios. A total of 536, $(N-1)$ contingencies are simulated for the 21 study cases described Section II, which sum to a total of 11 084 data sets (regressors), including the cases with no contingencies. The corresponding BCIs are calculated for each bus, of the 2418 bus within the system. To better understand the characteristics of the system studied, the histogram of the p_{critical} values of the system buses are plotted in Fig. 9 for the historical data derived from the contingency analysis.

As seen from Fig. 9, the probability of criticality for the 2418 buses considered in the studied system is mostly distributed between two ranges of [0, 0.1] and [0.9, 1]. The histogram of the average bus voltage magnitudes is presented in Fig. 10. As seen from Fig. 10 and explained in [3], due to the fact that the system is operating at 40% PV penetration, many system buses are operating at higher voltages particularly during some contingencies.

Comparing Figs. 9 and 10, it is observed that with the exception of a certain number of test cases, the system exhibits significant voltage magnitude violations for other cases. This observation confirms the results of the transient analysis presented in the previous section: there exists a DR at which the system demonstrates a more desirable behavior. Next, the steps shown in Fig. 8 are followed to calculate the ODR value for the system. The weight matrix W is calculated for two different

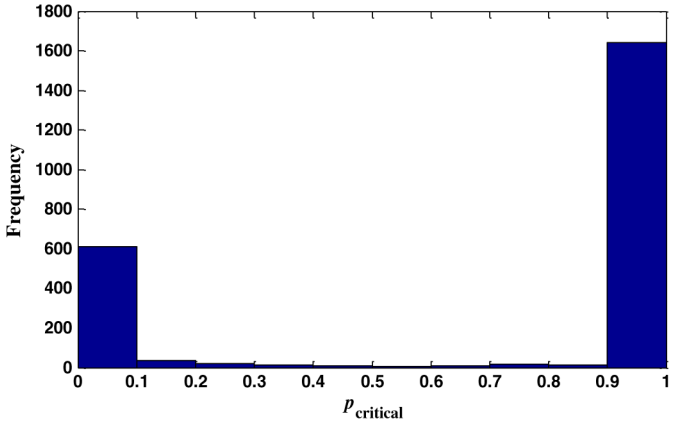

Fig. 9. Histogram for p_{critical} for the 2418 buses within the system.

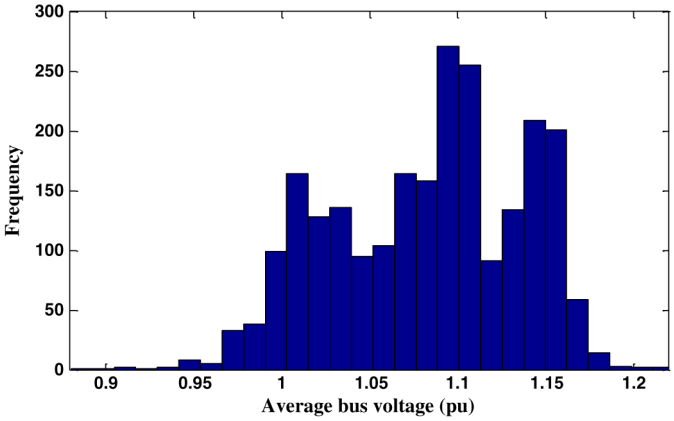

Fig. 10. Average bus voltage magnitude probability density for the 2418 buses within the system.

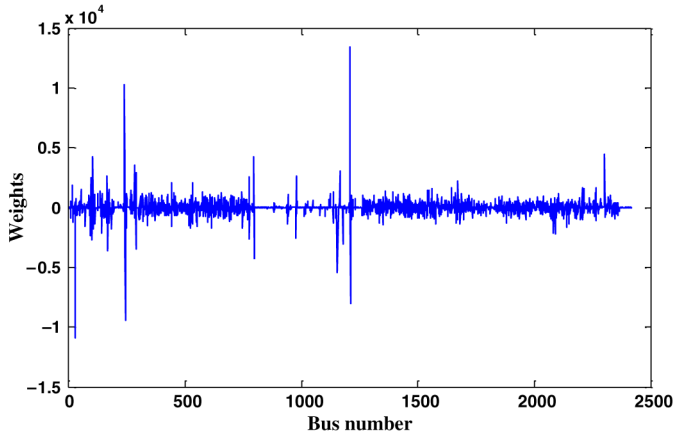

Fig. 11. Regression coefficients for BCIs calculated based on (3).

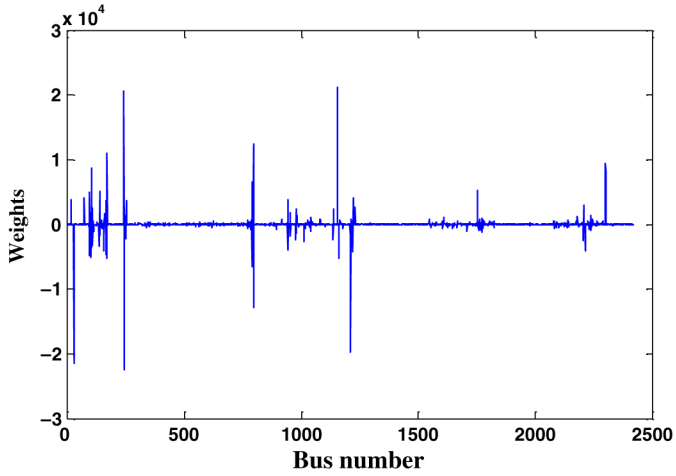

Fig. 12. Regression coefficients for BCIs calculated based on (7).

methods of calculating BCIs and the DR is estimated based on the bus BCI values. The elements of W are presented in Figs. 11 and 12 for two definitions of BCIs presented in (3) and (7).

The regression coefficients presented in Figs. 11 and 12 show that the output variable, i.e., DR, is more dependent on few BCIs rather than all the buses within the system. This phenomenon in effect, filters out the buses that are not affected under various DRs. Based on the regression coefficients derived from the test data, the ODR value is calculated to be 89.77% and 75.33% for BCI values based on, (3) and (7), respectively.

As explained before, (3) yields more conservative BCI values; therefore, fewer buses are filtered out in calculation of the BCI values, while (7) yields BCIs that are calculated based on the upper bound value of criticality. In this particular case and due to the large number of system buses, the small variations as shown in Fig. 11 will cause more errors to accumulate and result in larger ODR values. Consequently, the ODR calculated by (7) is selected because of the effectiveness of this method in eliminating the noncritical buses.

The criticality index can also be defined based on the steady-state power flows of the system transmission lines. Equation (3) is modified to define the line criticality index (LCI) of each transmission line based on the line flow

$$\text{LCI} = \left[3\int_0^p x^2 dx\right](1 + (1 - p_{\text{OverLimit}})g) \quad (16)$$

$$p_{\text{OverLimit}} = \frac{n_{\text{OverLimit}}}{n_{\text{OverLimit}} + n_{\text{UnderLimit}}} \quad (17)$$

$$g = u(p - P_{\text{lim}}) \quad (18)$$

where

p	line flows;
$n_{\text{OverLimit}}$	number of times the line flows are above the line MVA limit;
$n_{\text{UnderLimit}}$	number of times the line flows are below the line MVA limit.

Function $u(p - P_{lim})$ is a step function that equals to one if $p \geq P_{\text{lim}}$ and is zero otherwise.

Similar to (7), the LCI values can also be defined based on *Chebyshev's* theorem. The same procedure and data set introduced for the bus voltages can be applied to the calculation of ODR values based on the line flows. The regression coefficients for the LCI values calculated based on (16) are presented in Fig. 13. Following the same procedure as the bus voltages and calculating the ODR values for the test case that minimizes the system SCI, the ODR is found to be 71.64% based on (16) and

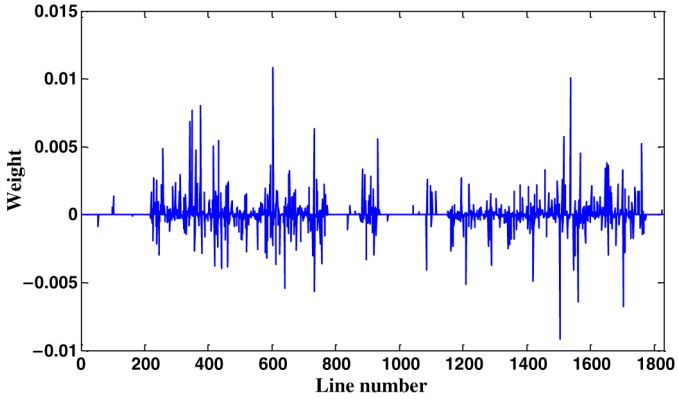

Fig. 13. Regression coefficients for LCIs calculated based on (16).

71.39% based on *Chebyshev's* theorem, which is very similar in both cases. The reason for this similarity is that, unlike bus voltages, the line flows generally are only affected if there is an outage in vicinity of any line. Therefore, the upper bound criticality defined by *Chebyshev's* theorem and $P_{\mathrm{OverLimit}}$ is in fact very close.

Finally, to determine the ODR that ensures a reliable performance based on steady-state bus voltages, steady-state line flows and transient response the maximum of the calculated ODR values is selected. For the studied system and a 40% PV penetration level, the calculated ODR that yields the aforementioned optimal performance is 75%. This means that for every 100 MW of PV addition to the system, 25 MW of generation is compensated by displacing conventional units and 75 MW of generation is compensated by a reduction in the generated output of the in-service units.

VI. Conclusion

This paper studied a real-world power system with high penetration PV generation to determine the ODR that ensures the stability of the system under various contingencies. A method for calculating the ODR was introduced and this ratio is mainly based on the steady-state behavior of the power system. Using regression techniques, this method utilizes a collection of test data in order to estimate the DR of the system as a function of BCIs that were also introduced in this paper. Simulation results of the contingency analysis identified the ODR with regards to steady-state bus voltages as well as line power flows. The ODR that yields acceptable transient behavior under various disturbances was also found based on simulation results.

Studies illustrate that various DRs can have diverse effects on steady-state and transient stability of the system. Therefore, to achieve reliability and maintain the stability of the system during various disturbances, it is essential to identify the ODR of the conventional generating units while the system is operating with high PV penetration. A measure of bus criticality or line criticality, concepts introduced in this work, effectively estimates the criticality of the system based on historical data obtained from contingency analysis. By calculating these indices, a linear regression-based method estimates the ODR as a function of the criticality indices. These methods provide a tool that can be applied to power systems prior to the addition of PV resources. The procedure is recommended to identify the ODR that eventually lead to fewer voltage instability or limit violations under contingencies.

References

[1] Center for Climate and Energy Solutions, *Renewable and Alternative Energy Portfolio Standards* [Online]. Available: http://www.c2es.org/node/9340

[2] (2003 Oct.). *IEEE 1547 Standard for Interconnecting Distributed Resources With Electric Power Systems*, IEEE [Online]. Available: http://grouper.ieee.org/groups/scc21/1547/1547_index.html

[3] S. Eftekharnejad, V. Vittal, G. T. Heydt, B. Keel, and J. Loehr, "Impact of increased penetration of photovoltaic generation on power systems," *IEEE Trans. Power Syst.*, vol. 28, no. 2, pp. 893–901, Apr. 2013.

[4] P. P. Barker and R. W. De Mello, "Determining the impact of distributed generation on power systems: Part I radial distribution systems," in *Proc. IEEE Power Eng. Soc. Summer Meet.*, Seattle, WA, USA, Jul. 2000, vol. 3, pp. 1645–1656.

[5] Y. Liu, J. Bebić, B. Kroposki, J. de Bedout, and W. Ren, "Distribution system voltage performance analysis for high penetration PV," in *Proc. IEEE Energy 2030 Conf.*, Atlanta, GA, USA, Nov. 2008, pp. 1–8.

[6] K. Turitsyn, P. Šulc, S. Backhaus, and M. Chertkov, "Distributed control of reactive power flow in a radial distribution circuit with high photovoltaic penetration," in *Proc. IEEE Power Energy Soc. Gen. Meet.*, Minneapolis, MN, USA, Jul. 2010, pp. 1–6.

[7] GE Energy, "Western wind and solar integration study: February 2008–February 2010 Feb," Nat. Renew. Energy Lab., Golden, CO, USA, Rep. SR-550-47434, May 2010.

[8] N. W. Miller, M. Shao, and S. Venkataraman, "California ISO (CAISO) frequency response study," in *Stakeholder Conf.* Schenectady, NY, USA: GE Energy, Nov. 2011.

[9] H. H. Happ, "Optimal power dispatch," *IEEE Trans. Power App. Syst.*, vol. PAS-93, no. 3, pp. 820–830, May 1974.

[10] J. Catalao, *Electric Power Systems: Advanced Forecasting Techniques and Optimal Generation Scheduling*, Boca Raton, FL, USA: CRC Press, Mar. 2012.

[11] Q. Ye, E. E. Zju, T. Ma, Y. Gu, and T. Wang, "Research on dispatch scheduling model of micro-grid with distributed energy," in *Proc. China Int. Conf. Elect. Distrib.*, Shanghai, China, Sep. 2012, pp. 1–5.

[12] J. Ma, S. Lu, P. V. Etingov, and Y. V. Makarov, "Evaluating the impact of solar generation on balancing requirements in Southern Nevada system," in *Proc. IEEE Power Energy Soc. Gen. Meet.*, San Diego, CA, USA, Jul. 2012, pp. 1–7.

[13] L. Xie and M. D. Ilić, "Model predictive dispatch in electric energy systems with intermittent resources," in *Proc. IEEE Int. Conf. Syst. Man Cybern.*, Singapore, Oct. 2008, pp. 42–47.

[14] North American Electric Reliability Corporation. (2008). *Standard BAL-001-0.1a: Real Power Balancing Control Performance* [Online]. Available: http://www.nerc.com/files/BAL-001-0_1a.pdf

[15] D. Knuth, *The Art of Computer Programming: Fundamental Algorithms*, vol. 1. Reading, MA, USA: Addison-Wesley, 1997.

[16] P. Chebyshev, "Des valeurs moyennes," *J. Math. Pures Appl.*, vol. 2, no. 12, pp. 177–184, 1867.

[17] C. M. Bishop, *Pattern Recognition and Machine Learning*, vol. 4. New York, NY, USA: Springer, 2006.

Sara Eftekharnejad (SM'12–M'13) received the B.Sc. degree from the University of Tehran, Tehran, Iran, in 2006, the M.Sc. degree from West Virginia University, Morgantown, WV, USA, in 2008, and the Ph.D. degree from Arizona State University, Tempe, AZ, USA, in 2012, all in electrical engineering.

She is currently with Tucson Electric Power (TEP), Tucson, AZ, USA.

Gerald Thomas Heydt (S'62–M'64–SM'80–F'91–LF'08) is from Las Vegas, NV, USA. He received the Ph.D. degree in electrical engineering from Purdue University, West Lafayette, IN, USA, in 1970.

His industrial experience is with the Commonwealth Edison Company, Chicago, IL, USA, and E.G.&G., Mercury, NV, USA. Currently, he is the Site Director of the Power Engineering Center Program, Arizona State University, Tempe, AZ, USA, where he is a Regents' Professor. He is also a Site Director of a new NSF Engineering Research Center on Future Renewable Electric Energy Delivery and Management (FREEDM) Systems.

Dr. Heydt is a member of the National Academy of Engineering. He is the recipient of the IEEE 2010 Richard H. Kaufmann Award.

Vijay Vittal (SM'78–F'97) received the B.E. degree from the B.M.S. College of Engineering, Bangalore, KA, India, in 1977, the M.Tech. degree from the Indian Institute of Technology, Kanpur, Kanpur, UP, India, in 1979, and the Ph.D. degree from Iowa State University, Ames, IA, USA, in 1982, all in electrical engineering.

Currently, he is the Director of the Power Systems Engineering Research Center (PSerc) and is the Ira A. Fulton Chair Professor with the Department of Electrical Engineering, Arizona State University, Tempe, AZ, USA.

Dr. Vittal is a member of the National Academy of Engineering.